Publications directly related to the content of this thesis:

I. **Szalárdy, L.**; Zádori, D.; Plangár, I., Vécsei, L.; Ludolph, AC, Weydt, P.; Klivényi, P.; Kovács GG. Neuropathology of partial PGC-1α deficiency recapitulates features of mitochondrial encephalopathies but not of neurodegenerative diseases. *Neurodeg. Dis.* **2013**, *12*(4):177–188. (IF: 3.454)

II. **Szalárdy, L**; Molnár, M; Török, R; Zádori, D; Vécsei, L; Klivényi, P; Liberski, PP; Kovács, GG. Histopathological comparison of Kearns-Sayre syndrome and PGC-1α-deficient mice suggests a novel concept for vacuole formation in mitochondrial encephalopathy. *Folia Neuropathol.* **2016**, *54*(1):9-22. (IF: 1.233)

Publications not directly related to the content of this thesis:

III. Török, N; Majláth, Z; **Szalárdy, L.**; Vécsei, L. Investigational α-synuclein aggregation inhibitors: hope for Parkinson's disease. *Expert Opin. Investig. Drugs* **2016**, In press. (IF: 4.408)

IV. **Szalárdy, L.**; Molnár, M.; Török, R.; Zádori, D.; Kovács, GG.; Vécsei, L; Klivényi, P. Lack of age-related clinical progression in PGC-1α-deficient mice - implications for mitochondrial encephalopathies. *Behav. Brain Res.* **2016**, 313:272-281. (IF: 3.002)

V. Molnár, FM; Török, R; **Szalárdy, L**; Sümegi, E; Vécsei, L; Klivényi, P. High-dose 1,25-dihydroxyvitamin D supplementation elongates the lifespan of Huntington's disease transgenic mice. *Acta Neurobiol. Exp.* **2016**, 76:176–181. (IF: 1.708)

VI. **Szalárdy, L**; Zádori, D; Klivényi, P; Vécsei, L. The role of CSF biomarkers in the evolution of diagnostic criteria in Alzheimer's disease: shortcomings in prodromal diagnosis. *J. Alzheimers Dis.* **2016**, 53(2):373–392. (IF: 3.920)

VII. Zádori, D; Veres, G; **Szalárdy, L**; Klivényi, P; Fülöp, F; Toldi, J; Vécsei; L. Inhibitors of the kynurenine pathway as neurotherapeutics: a patent review (2012-2015). *Expert Opin. Ther. Pat.* **2016**, 26(7):815–832. (IF: 4.626)

VIII. **Szalárdy, L**; Zádori, D; Klivényi, P; Toldi J., Vécsei, L. Electron transport disturbances and neurodegeneration: from Albert Szent-Györgyi's concept (Szeged) till novel approaches to boost mitochondrial bioenergetics. *Ox. Med. Cell. Longev.* **2015**, 2015:498401. (IF: 4.492)

IX. Zádori, D; Veres, G; **Szalárdy, L**; Klivényi, P; Vécsei, L. Drug-induced movement disorders. *Expert Opin. Drug Saf.* **2015**, *14*(6):877–890. (IF: 2.896)

X. Veres, G; Molnár, M; Zádori, D; Szentirmai, M; **Szalárdy, L**; Török, R; Fazekas, E; Ilisz, I; Vécsei, L; Klivényi, P. Central nervous system-specific alterations in tryptophan metabolism in 3-nitropropionic acid model of Huntington's disease. *Pharmacol. Biochem. Behav.* **2015**, 132:115–124. (IF: 2.537)

XI. Török, R.; Kónya, JA; Zádori, D; Veres, G; **Szalárdy, L**; Vécsei, L; Klivényi, P. mRNA expression levels of PGC-1α in a Transgenic and a toxin model of Huntington's disease. *Cell. Mol. Neurobiol.* **2015,** *35*(2):293–301. (IF: 2.328)

XII. Grozdics, E; Berta, L; Gyarmati, B; Veres, G; Zádori, D; **Szalárdy, L**; Vécsei, L; Tulassay, T; Toldi, G. B7 costimulation and intracellular indoleamine 2,3-dioxygenase expression in umbilical cord blood and adult peripheral blood. *Biol. Blood Marrow Transplant.* **2014**, *20*(10):1659–1665 (IF: 3.404)

XIII. Zádori, D; Veres, G; **Szalárdy, L**; Klivényi, P; Toldi, J; Vécsei, L. Glutamatergic dysfunctioning in Alzheimer's disease and related therapeutic targets. *J. Alzheimers Dis.* **2014**, *42*(Suppl 3):S177–187. (IF: 4.151)

XIV. Plangár, I; Zádori, D; **Szalárdy, L**; Vécsei, L; Klivényi, P. Assessment of the role of multidrug resistance-associated proteins in MPTP neurotoxicity in mice. *Ideggyogy. Sz.* **2013**, *66*(11–12):407–414. (IF: 0.343)

XV. **Szalárdy, L**; Zádori, D; Tánczos, E; Simu, M; Bencsik, K; Vécsei, L; Klivényi, P. Elevated levels of PPAR-gamma in the cerebrospinal fluid of patients with multiple sclerosis. *Neurosci. Lett.* **2013**, *554*:131–134. (IF: 2.055)

XVI. Török, R; Török, N; **Szalárdy, L**; Plangár, I; Szolnoki, Z; Somogyvári, F; Vécsei, L; Klivényi, P. Association of vitamin D receptor gene polymorphisms and Parkinson's disease in Hungarians. *Neurosci. Lett.* **2013**, *551*:70–74. (IF: 2.055)

XVII. **Szalárdy, L**; Zádori, D; Simu, M; Bencsik, K; Vécsei, L; Klivényi, P. Evaluating biomarkers of neuronal degeneration and neuroinflammation in CSF of patients with multiple sclerosis - osteopontin is a potential marker of clinical severity. *J. Neurol. Sci.* **2013**, *331*(1–2):38–42. (IF: 2.262)

XVIII. Zádori, D; **Szalárdy, L**; Toldi, J; Fülöp, F; Klivényi, P; Vécsei, L. Some molecular mechanisms of dopaminergic and glutamatergic dysfunctioning in Parkinson's disease. *J. Neural Transm.* **2013**, *120*(4):673–81. (IF: 2.871)

XIX. Vécsei, L; **Szalárdy, L**; Fülöp, F; Toldi, J. Kynurenines in the CNS – recent advances and new questions. *Nat. Rev. Drug. Discov.* **2013**, *12*(1), 64–82. (IF: 37.231)

XX. **Szalárdy, L**; Zádori, D; Fülöp, F; Toldi, J, Klivényi, P; Vécsei, L. Manipulating kynurenic acid levels in the brain – on the edge between neuroprotection and cognitive dysfunction. *Curr. Top. Med. Chem.* **2012**, *12*(16), 1797–1806. (IF: 3.702)

XXI. Zádori, D; Klivényi, P; **Szalárdy, L**; Fülöp, F; Toldi, J; Vécsei, L. Mitochondrial disturbances, excitotoxicity, neuroinflammation and kynurenines: novel therapeutic strategies of neurodegenerative disorders. *J. Neurol. Sci.* **2012**, *322*(1–2), 187–191. (IF: 2.243)

XXII. Vécsei, L; Plangár, I, **Szalárdy, L.** Manipulation with the kynurenines – a possible tool for treating neurodegenerative diseases? *Exp. Rev. Clin. Pharm.* **2012**, *5*(4), 351–353. (editorial)

XXIII. **Szalárdy, L**; Klivényi, P; Zádori, D; Fülöp, F; Toldi, J; Vécsei, L. Mitochondrial disturbances, tryptophan metabolites and neurodegeneration: medicinal chemistry aspects. *Curr. Med. Chem.* **2012**, *19*(13), 1899–1920. (IF: 4.070)

Cumulative impact factor: **98.991**

I. INTRODUCTION

Several lines of evidence obtained in the past decade suggest that peroxisome proliferator-activated receptor-gamma (PPARγ) coactivator 1-alpha (PGC-1α), a nuclear-encoded coactivator of a wide range of transcriptional factors, plays a key role in the transcriptional cascade of processes involved in adaptive mitochondrial biogenesis. PGC-1α-mediated coactivation of genes such as nuclear respiratory factor 1 and 2 (NRF-1 and -2), PPARs, estrogen-related receptors (ERRs), myocyte-specific enhancer factor 2C (MEF2C) leads to an increased expression of a spectrum of proteins involved in mitochondrial transcription, replication, the import and assembly of a number of nuclear-encoded respiratory complex subunits; furthermore, it boosts oxidative phosphorylation and thermoregulation in a tissue-dependent manner, enhances gluconeogenesis and fatty acid oxidation, and increases the defense against oxidative stress (Figure 1).

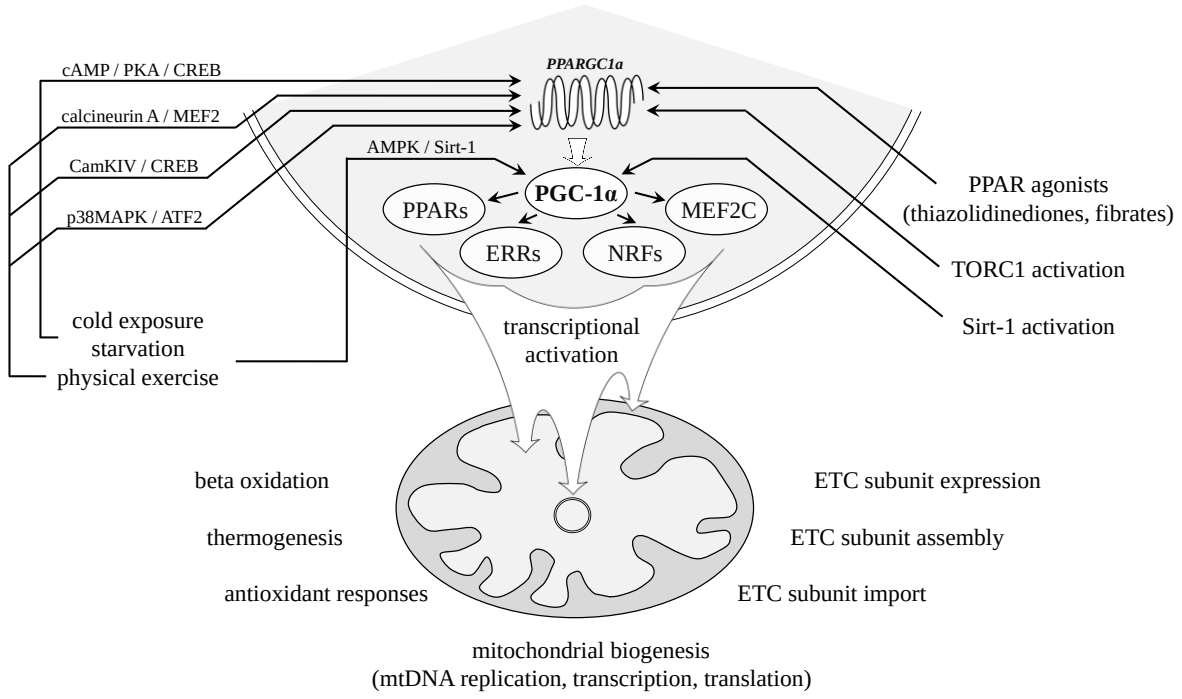

Figure 1. The PGC-1α cascade. Transcriptional upregulation or posttranslational activation of PGC-1α due to fasting, physical exercise, cold exposure, or pharmacological manipulations lead to the transcriptional activation several nuclear-encoded proteins involved in mitochondrial functioning at multiple levels, including mitochondrial biogenesis, adaptive metabolism, antioxidant responses, and proper electron transport chain (ETC) assembly/import.

A number of observations explain the special susceptibility of the central nervous system (CNS) to suffer injuries due to mitochondrial disturbances, including the extreme high energy demand and the need of constant glucose and oxygen availability of neurons. This is in line with the armada of observations placing mitochondrial dysfunction in the center of disease pathogenesis in a variety of neurodegenerative disorders, including Alzheimer's disease (AD), Parkinson's disease (PD), Huntington's disease (HD), and amyotrophic lateral sclerosis (ALS) [29]. In neurodegenerative diseases, the progressive loss of neurons in particular regions of the CNS is accompanied by the dysfunctional degradation and subsequent aggregation of misfolded proteins such as hyperphosphorylated Tau (pTau), amyloid-β (Aβ), α-synuclein, trans-activation response (TAR) DNA-binding protein (TDP-43), and fused in sarcoma protein (FUS). Emerging evidence suggests that mitochondrial dysfunction and impaired protein processing in such conditions are closely interrelated. In addition to the well-known sensitivity of neurons as opposed to the relative resistance of astrocytes to oxygen or glucose deprivation, recent studies suggest that oligodendrocytes are among the most sensitive cell types within the CNS to mitochondrial stress, exceeding the vulnerability of neurons, a feature which may have implications for the pathogenesis of characteristic myelinopathies in chronic conditions with mitochondrial dysfunction, including aging and mitochondrial encephalopathies.

A series of evidence suggests that a deficient function of the PGC-1α axis may play an important role in mitochondrial dysfunction and hence protein aggregation in neurodegenerative diseases. Indeed, an inverse correlation of hippocampal PGC-1α protein content with the severity of neuritic plaque pathology and hippocampal $A\beta_{x-42}$ burden has been reported in AD patients, with *in vitro* evidence suggesting that PGC-1α deficiency might decrease non-amyloidogenic α-secretase activity. Furthermore, a genome-wide analysis found 425 PGC-1α-responsive nuclear-encoded mitochondrial genes underexpressed in sporadic PD, and PGC-1α single nucleotide polymorphisms (SNPs) have been associated with the risk and age of onset of PD, corresponding with a decreased expression of PGC-1α in the affected brain regions of PD patients and conditional parkin knockout mice. Importantly, the reduced expression of PGC-1α enhances α-synuclein oligomerization *in vitro*. As regards, HD, downregulated PGC-1α expression was found of in the striatum of HD patients, in transgenic HD animals, and in *in vitro* HD models. Correspondingly, the decreased expression of several PGC-1α target genes have been identified in the striatum of HD patients and transgenic HD mice. Polymorphisms in the PGC-1α gene were found to modify the age at onset of HD.

Though no mutations of PGC-1α have been directly associated with inherited mitochondrial disease, considering that a number of genes involved in disease-causing mutations and/or in modeling mitochondrial disease have direct or indirect interactions with PGC-1α, the rationale for PGC-1α induction to provide symptomatic benefit in this currently intractable group of diseases can be accepted, and is supported by a number of experimental studies in models of mitochondrial cytopathies.

PGC-1α-deficient animals – intriguing contradictions

PGC-1α has recently been described to undergo an alternative 3' splicing between exons 6 and 7, which produces an in-frame stop codon at amino acid 268, resulting in a shorter but functionally active splice variant of PGC-1α called N-truncated or N-terminal fragment of PGC-1α (NT-PGC-1α; comprising 267 amino acids). In the past years, two independently developed whole-body knockout murine strains of PGC-1α have been generated. The first strain represents a complete knockout of PGC-1α (PGC-1α -/-), whereas the parallel-developed strain lacks the expression of the full-length protein (FL-PGC-1α -/-) but readily expresses a slightly shorter but functional form of the splice variant NT-PGC-1α, denoted as NT-PGC-1α^{254}. Notably, both PGC-1α whole-body knockout strains were reported to display astrogliosis and tissue vacuolation in the brain, predominantly in the striatum, which led to the conclusion that PGC-1α deficiency may model neurodegeneration, more particularly HD. Intriguingly, the complete PGC-1α -/- mice were reported to exert hyperactivity and was interpreted as HD-like hyperkinetic phenotype; whereas, contrastingly, FL-PGC-1α -/- mice exhibit hypomotility and weakness.

II. OBJECTIVES

Based on the concordant data linking mitochondrial dysfunction and PGC-1α deficiency to the dysregulation of neuronal protein processing and handling in neurodegenerative disorders, we performed a systematic neuropathological characterization of FL-PGC-1α -/- mice, with special focus on the immunohistochemical pattern of neurodegeneration-related proteins. As neither brain vacuolation nor hyperkinetic behavior is typical feature of transgenic or systemic toxin-induced model mice of HD, our aim was to create a comprehensive neuropathological lesion profile of FL-PGC-1α -/- animals. Since the initial results linked the neuropathological phenotype to mitochondrial disease, samples of old animals were systematically compared with human brain tissue samples from a case with definite mitochondrial encephalopathy.

III. MATERIALS AND METHODS

FL-PGC-1α -/- mice were generated in Kelly Lab and bred in our Department. Histopathological examinations were performed at two age groups, at 30 and 70-75-weeks of age. Immunohistochemical analysis of neurodegeneration-related proteins in sagittal, paraffin-embedded brain sections included staining against ubiquitin, Tau, pTau (AT8), α-synuclein, Aβ, APP, prion protein (epitope 144-152), TDP-43, and FUS. Neuropathological profiling was performed by the use Hematoxylin and Eosin (H&E), Klüver-Barrera, Oil Red O, and Bielschowsky silver stainings, and immunohistochemistry for glial fibrillary acidic protein (GFAP), TPPP/p25 (a marker of mature oligodendrocytes), phosphorylated and non-phosphorylated neurofilaments (SMI-31 and SMI-32) and microtubule-associated protein-2 (MAP-2) as neuronal markers, myelin basic protein (MBP), and Iba1 (a microglia marker). Neuropathological profiling was also performed on sections from a genetically confirmed case of KSS (male patient, died at 22 years of age). Vacuolation and astrogliosis in the mice were semiquantitatively evaluated (Figure 2). Specimens prepared for electron microscopy were examined using a JEM-100C transmission electron microscope. Statistical analysis was performed by the use of Fisher's exact test where appropriate.

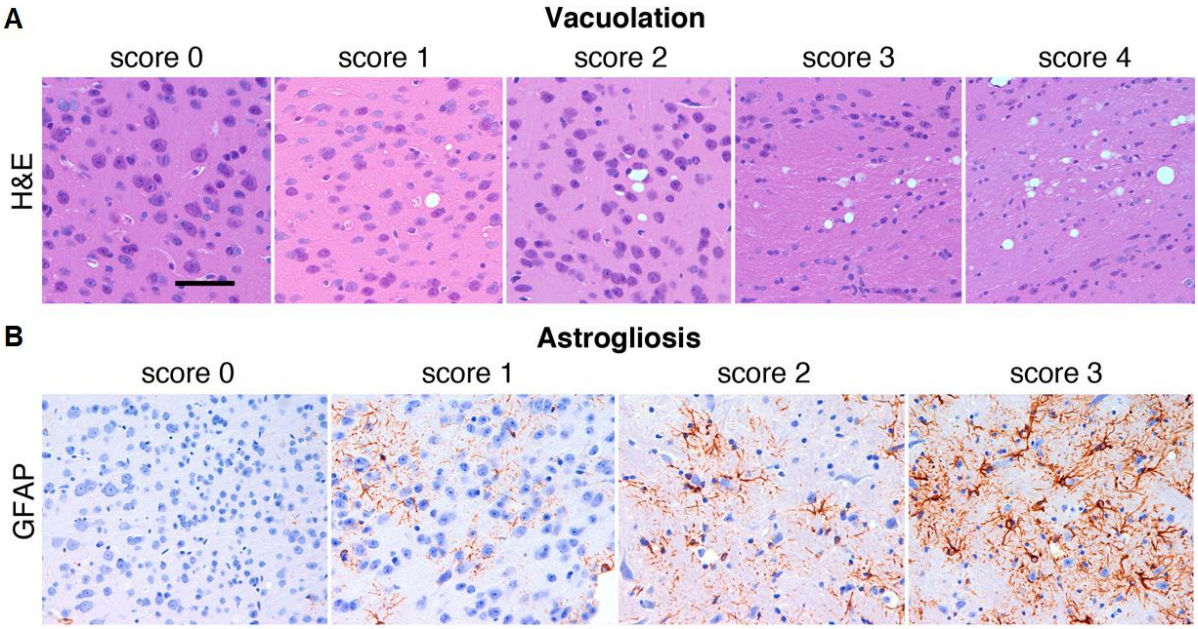

Figure 2. Representative images corresponding to the semiquantitative scores used to evaluate vacuolation (**A**) and astrogliosis (**B**) in FL-PGC-1α -/-. Bar in a represents 20 μm.

IV. RESULTS

IV.1. Immunostaining for neurodegeneration-related proteins

Immunostaining for prion protein (PrP), α-synuclein (a-Syn), amyloid precursor protein (APP), amyloid-beta (A-beta), Tau, pTau, TDP-43, FUS, and ubiquitin (Ubi) in various anatomical regions in wild-type (WT) and FL-PGC-1α -/- (PGC-1α) animals were performed. We observed the lack of pathological protein aggregation and inclusion body formation with physiological staining patterns throughout the brain of mature FL-PGC-1α -/- mice (Figure 3). This picture was virtually identical when examining 70-75-week-old FL-PGC-1α -/- mice in a subsequent experimental setting (data not shown).

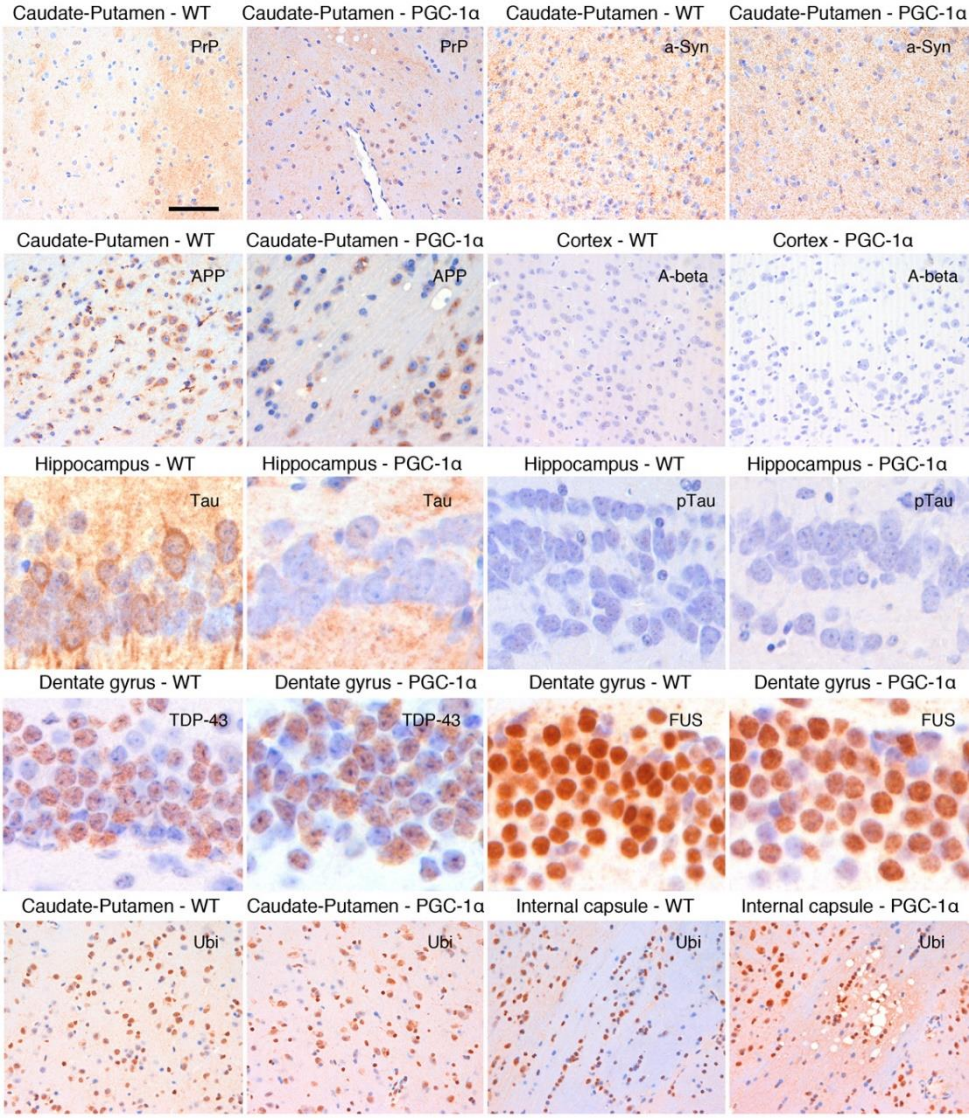

Figure 3. The absence of FL-PGC-1α expression is not associated with the accumulation of neurodegeneration-related proteins in 30-week old adult mice.

IV.2. Lesion profile analysis of adult FL-PGC-1α -/- mice

At 30 weeks of age, neuropathological changes in the mice included wide-spread vacuolation, predominantly in the WM, and reactive astrogliosis in certain brain regions.

The caudate-putamen was the most severely vacuolated GM structure (Table 1); vacuolation within the neocortex predominated in the deep cortical layers, and the spongy change in the pontomedullary brainstem was more severe in the paramedian sections (p = 0.018). Among the widely involved WM structures, the most severe vacuolation was observed in the internal capsule and the retroflex fascicle (Figure 4).

Typical degree of vacuolation	Region	Mean	*p*-value
Mild	cerebellar WM	*1.833*	*< 0.001*
	pontomedullary brainstem [l] *	*1.923*	*0.005*
	substantia nigra	*1.375*	*0.004*
	hippocampus [m]	*1.133*	*0.006*
	hippocampus [l]	*1.933*	*< 0.001*
	fimbria hippocampi	*1.182*	*0.007*
Moderate	cerebellar nuclei *	*2.150*	*< 0.001*
	pontomedullary brainstem [m] **	*2.933*	*< 0.001*
	midbrain *	*2.571*	*< 0.001*
	nucleus accumbens	*2.600*	*< 0.001*
	globus pallidus	*2.692*	*< 0.001*
	mammillary body	*2.143*	*< 0.001*
	cerebral cortex	*2.305*	*< 0.001*
	thalamus [m]	*2.067*	*< 0.001*
	anterior commissure	*2.533*	*< 0.001*
	stria terminalis	*2.786*	*< 0.001*
	olfactory tract	*2.071*	*< 0.001*
Severe	caudate-putamen	*4.000*	*< 0.001*
	thalamus [l]	*3.533*	*< 0.001*
	internal capsule	*3.615*	*< 0.001*
	retroflex fascicle	*4.000*	*< 0.001*

[l] lateral section; [m] paramedian section; * accompanied by moderate astrogliotic reaction; ** accompanied by severe astrogliotic reaction.

Table 1. Lesion profile in the brains of FL-PGC-1α -/- mice. Comprehensive mapping of lesion profile in FL-PGC-1α -/- animals, demonstrating the typical degree of involvement of an anatomical region in the spongiform vacuolation and reactive astrogliosis. The differences between FL-PGC-1α -/- and wild-type animals are represented by the means and the corresponding p values in the respective anatomical regions.

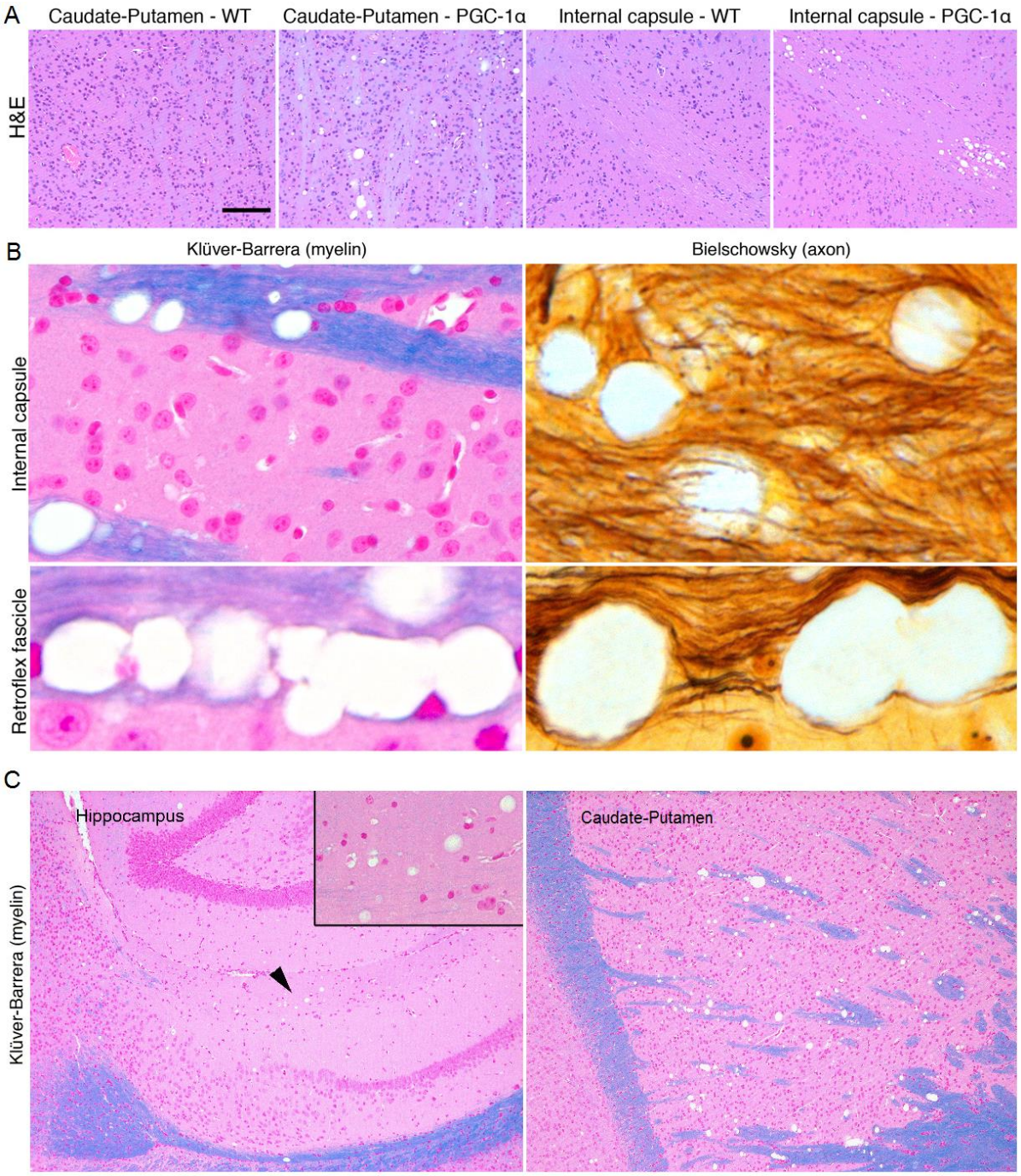

Figure 4. Vacuolation in the brains of adult FL-PGC-1α -/- mice is reminiscent of human mitochondrial leukoencephalopathies. (**A**) H&E staining in different anatomical regions in wild-type (WT) and FL-PGC-1α -/- (PGC-1α) animals demonstrates prominent vacuolation in the caudate-putamen and the internal capsule in FL-PGC-1α -/- animals. (**B**) Vacuolation in the WM (as shown by Klüver-Barrera staining on the middle left) often exhibits chain-like appearance and is associated with seemingly well-preserved axons, pushed towards the edge of the vacuoles (as shown by Bielschowsky silver staining on the middle right). (**C**) Vacuoles in the neuropil appear to associate with WM structures as revealed by Klüver-Barrera staining of the hippocampus (lacunosum molecular layer) and caudate-putamen (pencil fibers).

Indicative of chronic neuronal degeneration, prominent reactive gliosis was present in the brainstem and within the cerebellar nuclei of FL-PGC-1α -/- mice. This was the most striking in the paramedian sections of the pontomedullary brainstem, whereas moderate astrogliosis was noted in the midbrain, the cerebellar nuclei, and the lateral pontomedullary brainstem (Figure 5). The median predominance of the involvement of the pontomedullary brainstem was statistically significant (Fisher's exact value = 10.758; p = 0.004).

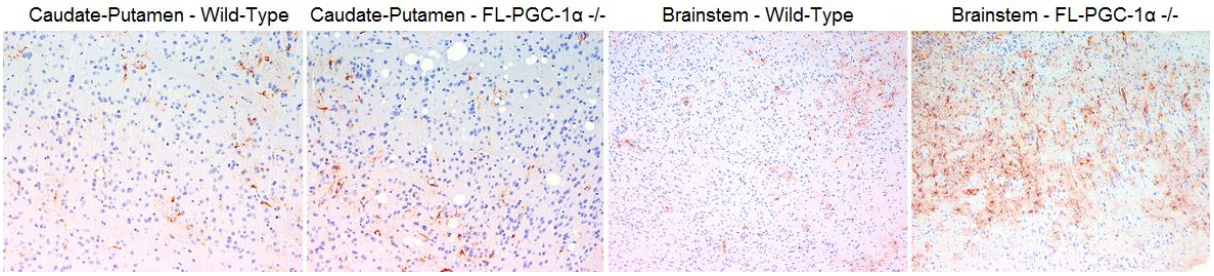

Figure 5. Immunostaining for GFAP showed reactive astrogliosis indicative of chronic neuronal degeneration in the pontomedullary brainstem and certain deep cerebellar nuclei but not in the caudate-putamen (as previously reported) of adult FL-PGC-1α -/- animals.

Concluding these initial results, the observed lesion profile did not recapitulate features characteristic of neurodegenerative diseases (including HD, AD, and PD) either in terms of impaired protein processing or the localization of signs of neuronal degeneration. However, with wide-spread vacuolation predominantly affecting the WM of the basal ganglia, thalamus, brainstem, and cerebellum, as well as reactive astrogliosis in the brainstem and deep cerebellar nuclei, the observed picture was remarkably reminiscent of that seen in mitochondrial spongiform leukoencephalopathies, in particular the KSS (Table 2). This prompted us to further explore and characterize the observed lesion profile in a systematic comparison of aged FL-PGC-1α -/- animals and a human brain with KSS by the use of further immunohistochemical and electron microscopic techniques, with a special focus on the origin of vacuoles.

IV.3. Comparison of lesion profiles between human KSS and aged FL-PGC-1α -/- mice

Vacuolation

Klüver-Barrera staining revealed widespread spongiform change in both the KSS brain and 70-75-week old aged FL-PGC-1α -/- mice. In both, the vacuolation predominated in the WM; however, vacuoles in the GM neuropil were also observed with apparently lower frequency (Figure 6A-F). The vacuolation commonly affected the internal capsule, striatal pencil fibers, cerebellar WM, thalamic fascicules, pyramidal tracts, and, less intensively, the corpus callosum. Vacuoles were commonly present in the neuropil, most intensively in the brainstem, but also consistently present in the basal ganglia, thalamic nuclei, and less intensively, in the neocortex, where they showed a predilection towards the deep cortical layers. The vacuolation was more prominent in the KSS brain than in experimental animals; in some regions with coarse cystic-necrotic lesions and myelin pallor, whereas in some others with demyelinated foci (*e.g.*, postcentral region, cerebellar WM, and some of the pencil fibers) (Figure 6C and F). Demyelination and cystic-necrotic lesions were undetected in FL-PGC-1α -/- mice. Notably, the examined aged wild-type brains presented vacuoles showing similar appearance and distribution as their FL-PGC-1α-deficient counterparts; however, their frequency was remarkably lower in all examined regions (Figure 6A-B and D-E).

Astrogliosis

GFAP staining revealed moderate-to-severe reactive astrogliosis in the brainstem and cerebellum of both the KSS and the FL-PGC-1α-deficient brains (Figure 6G-I). In the KSS brain, astroglial reaction was observed in the tectal midbrain, the area of the inferior olive in the medulla oblongata, the dentate nucleus of the cerebellum, and the Purkinje cell layer (*i.e.*, Bergmann gliosis). In the FL-PGC-1α-deficient mice, severe reaction was present in the medulla oblongata and the pons often in a confluent pattern involving large areas without being limited to certain groups of nuclei, whereas mild reaction with patchy astrocytosis was observed in the midbrain and in the deep cerebellar nuclei. Notably, the caudate-putamen of FL-PGC-1α -/- mice were free of astroglial reaction even at this age (Figure 7), supporting our prior observations.

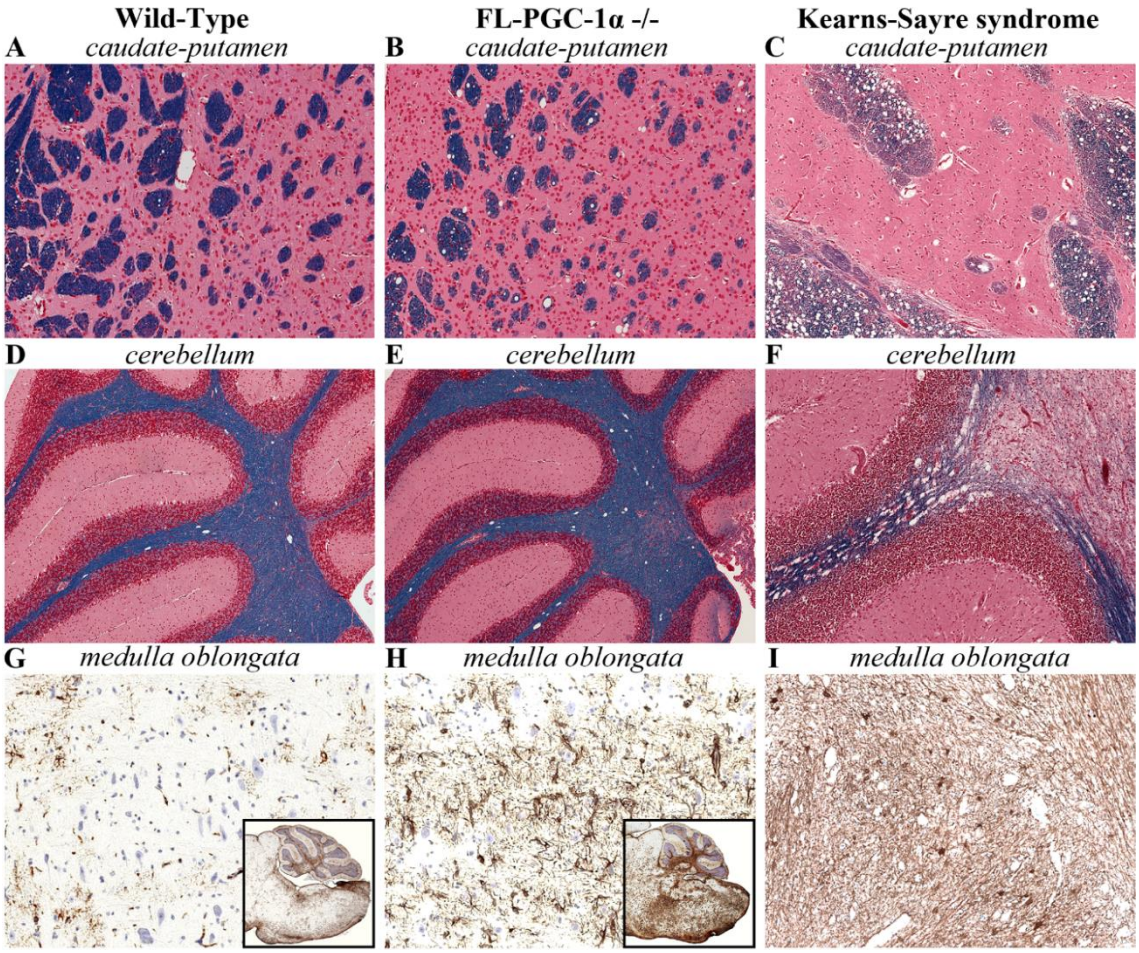

Figure 6. Vacuolation and astroglial reaction. Aged FL-PGC-1α-deficient mice develop moderate-to-severe vacuolation (**B** and **E**) in areas corresponding to severe-to-devastating vacuolation in KSS (**C** and **F**) and mild vacuolation in aged wild-type mice (**A** and **D**; Klüver-Barrera). Vacuoles are in association with WM structures. Note the patchy areas of myelin pallor in the pencil fibers of the caudate-putamen (**C**) and the demyelinated cystic-necrotic lesion in the cerebellar WM in KSS (**F**). Reactive astrogliosis indicative of neuronal degeneration is present in the brainstem of FL-PGC-1α-deficient mice and the KSS case (**H** and **I**; GFAP).

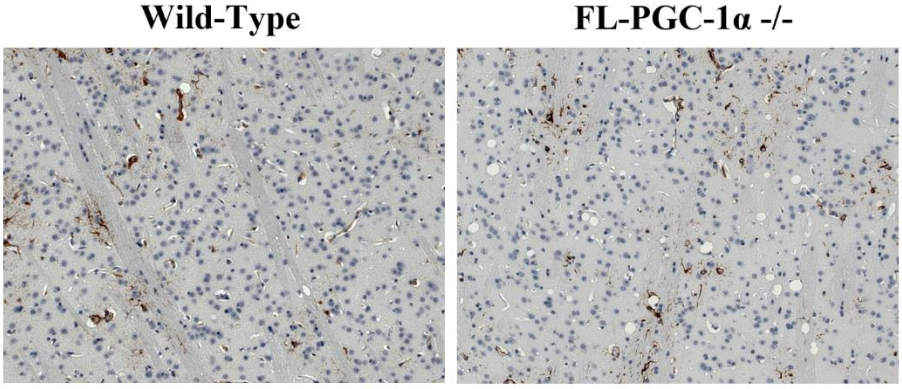

Figure 7. The caudate-putamen of FL-PGC-1α -/- mice is free of reactive astrogliosis (GFAP) even at 70-75 weeks of age, suggesting that this murine strain is not a model for HD, as it was previously suggested.

Axonal pathology

The intensity of axonal destruction in the KSS brain was variable and generally followed that of the vacuolar change. Only the severely affected cystic-necrotic lesions showed axonal loss or swelling, whereas most of the moderately vacuolated areas were devoid of axonal pathology (Figure 8C), except for scattered swellings and APP-positive spheroids indicating acute-subacute impairment of axonal transport (Figure 8F). Regions with severe axonal involvement were accompanied by reactive microgliosis (Figure 8I). The axons in FL-PGC-1α -/- mice were generally well preserved with patterns of APP, neurofilament and microglia stainings being similar to that seen in wild-type (Figure 8A-B, D-E, and G-H).

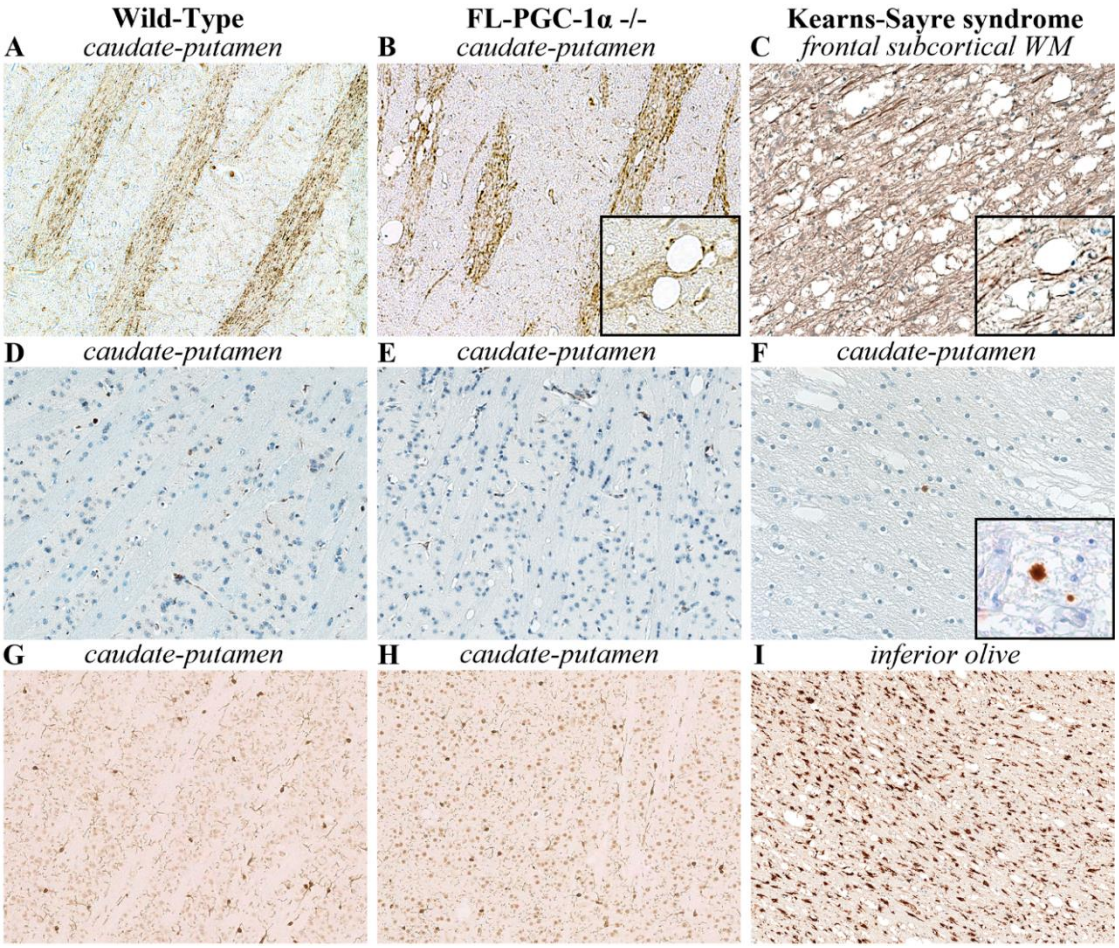

Figure 8. Axonal pathology. Axons in moderately vacuolated areas in KSS were relatively intact with scattered appearance of axonal swellings (**C**; SMI-31) and APP+ axonal spheroids indicative of subacute axonal transport impairment (**F**; APP). Regions with cystic-necrotic lesions showed robust microglia accumulation in KSS (**I**; Iba). These pathologies were virtually absent in the FL-PGC-1α -/- mice and the immunohistochemical patterns were rather similar to that in aged wild-types (**A-B**, **D-E**, and **G-H**). Note the well-preserved axons dodging between multiple vacuoles (**B**), similarly to that seen in KSS (**C**).

Characterization of white matter vacuoles

Vacuoles within the WM were surrounded by rings of MBP-positive myelin in both the KSS and FL-PGC-1α-deficient brains (Figure 9A). The vacuoles were usually ovoid with their longitudinal axis paralleling the direction of axons. They often formed chain-like structures in longitudinal or sieve-like lesions in transverse sections. No apparent macrophage activity was present even in the areas of severe vacuolation, and no signs of active myelin degradation could be detected by Oil Red O (not shown). Electron microscopy revealed that myelin 'bubbles' in the WM were formed mostly by splitting at the intraperiod lines (Figure 10A-B), and in the KSS material (where countless vacuoles could be analyzed) occurrences between the axons and the innermost myelin lamellae (adaxonal vacuoles) could also be noticed (Figure 11). The vacuoles were 'empty' or contained various amount of debris with myelin-like figures (Figure 10A-B, Figure 11).

Characterization of neuropil vacuoles

Staining for neuronal (MAP-2 and SMI-32) or astrocytic (GFAP) antigens sparsely revealed associations of neuropil vacuoles with these cell-types in either the KSS or the FL-PGC-1α-deficient brains (Figure 12). Staining for MBP, however, unveiled that the vast majority of neuropil vacuoles were clearly encompassed by a myelin-positive rim, suggesting a same intramyelinic localization as for vacuoles within the WM (Figure 9B). Neuropil vacuoles were also frequently associated with oligodendrocytes in sections immunostained for TPPP/p25 (Figure 9C). Such close contacts of oligodendrocytes and vacuoles were also observed by electron microscopy. Furthermore, vacuoles (sometimes multiloculated) could frequently be identified within the cytoplasm of glial cells, which, due to the lack of glial fibers observed in the cytoplasm, also appeared to be oligodendrocytic (Figure 10C). Likewise myelin 'bubbles', these membrane-bound vacuoles often contained myelin-like figures, and they occasionally coalesced occupying most of the oligodendroglial cytoplasm and led to the swelling of the cells (Figure 10C). These observations were seen in both the KSS and the FL-PGC-1α-deficient brains.

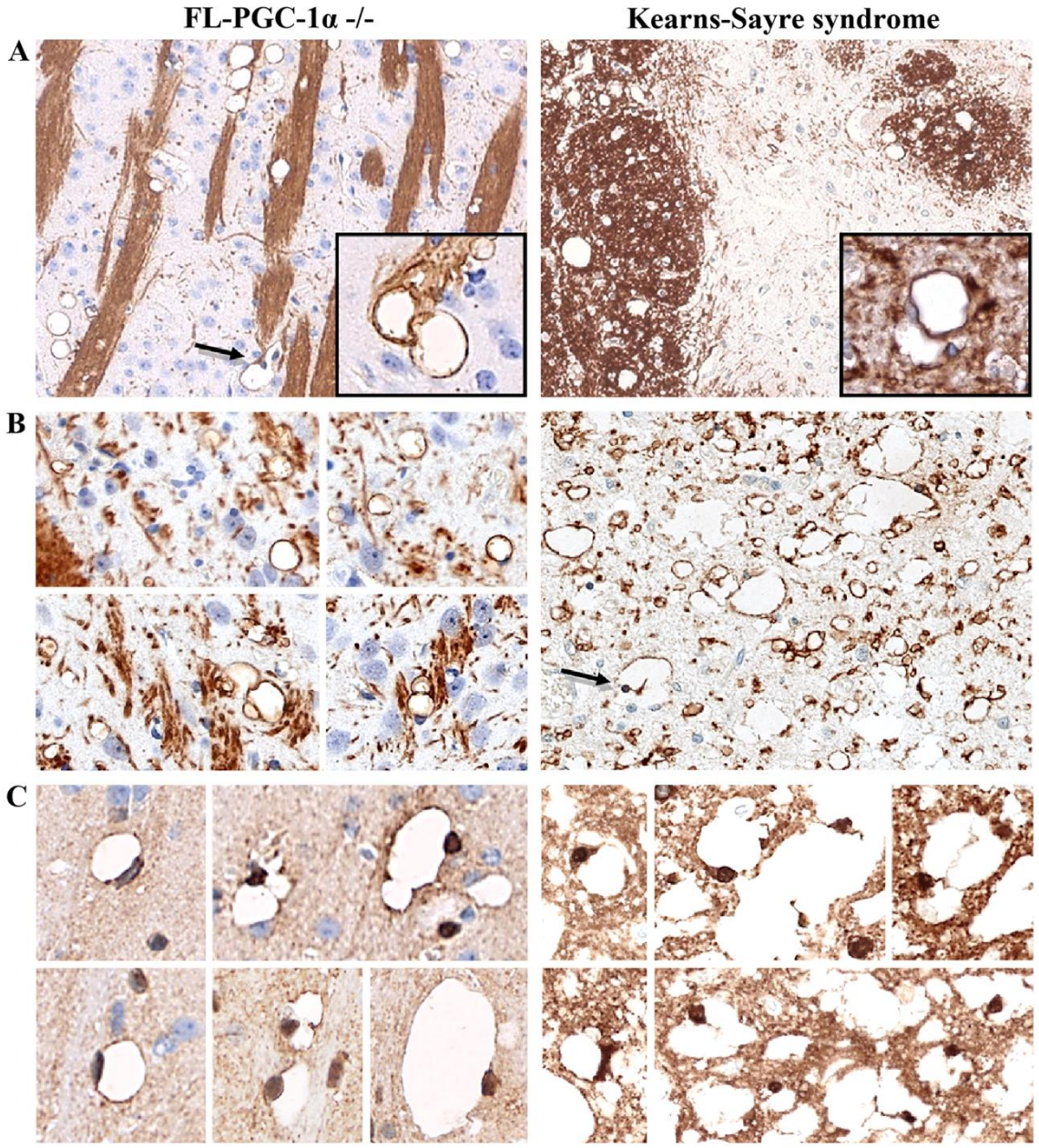

Figure 9. Immunohistochemical characterization of vacuoles. Vacuoles within the WM are surrounded by rings of myelin (**A**; MBP). Likewise WM myelin 'bubbles', vacuoles within the GM neuropil are also encompassed by a myelin-positive rim, suggesting an identical origin (**B**; MBP). Oligodendroglial cells in close contact with and/or localized within the inner edge of either single or multiloculated vacuoles can frequently be detected by immunohistochemistry (**C**; TPPP/p25), suggesting an important role of oligodendrocytes in vacuole formation. Note some of the larger vacuoles being separated to multiple chambers by oligodendroglial processes (**C**). Note also the glial cell encompassing a vacuole with its MBP+ process (indicated by arrows, **A** – left, **B** – right).

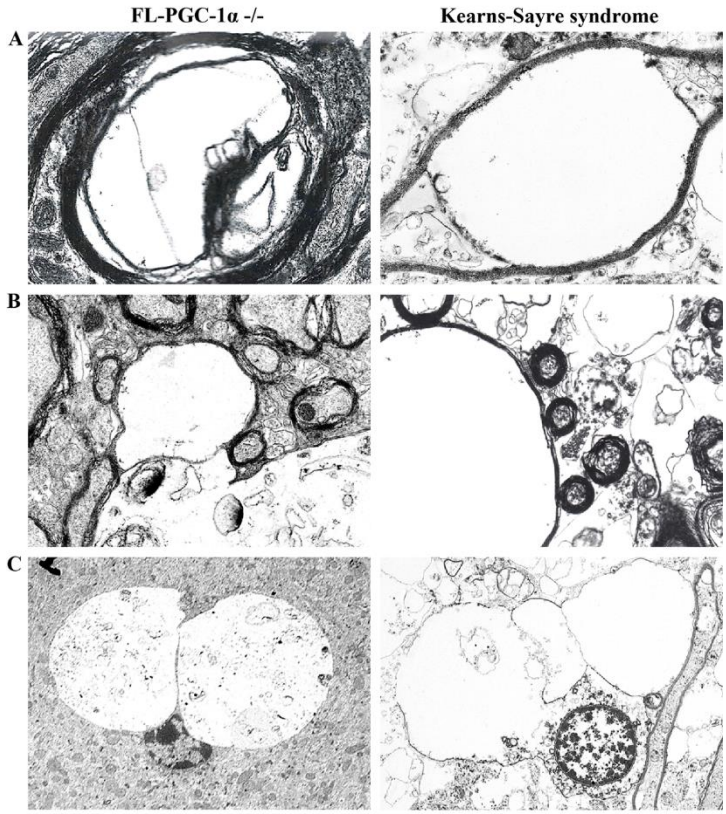

Figure 10. Ultrastructural characterization of vacuoles. Intramyelin vacuolation can be identified also by electron microscopy (longitudinal section, **A**; transverse section, **B**). In accordance with immune-histochemical findings, vacuoles, often multiloculated, can frequently be identified within the cytoplasm of oligodendroglial cells by electron microscopy (**C**). Oligodendroglial vacuoles have not been reported previously in mitochondrial encephalopathies, and their presence as a potential source of intramyelin vacuoles might underlie their focal appearance.

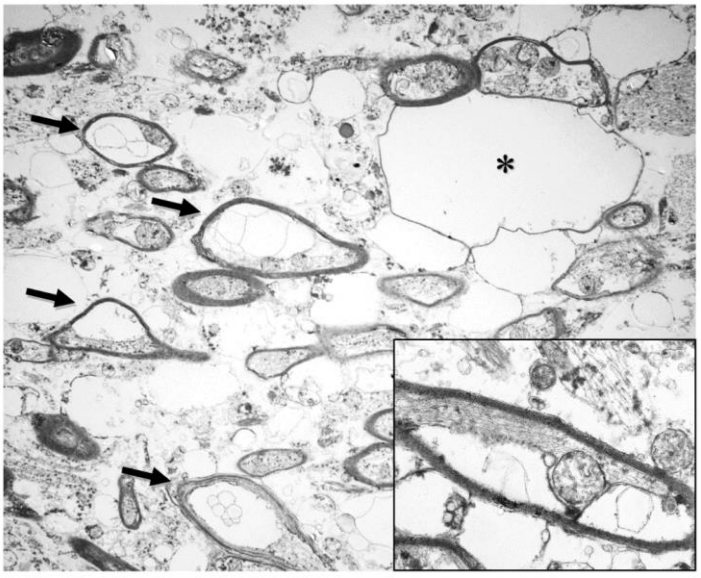

Figure 11. Distinct types of intramyelin vacuoles in KSS. Asterisk denotes a huge ’classical’ intramyelin vacuole originating from splitting at the intraperiod line. Arrows indicate the multiple presence of adaxonal vacuoles, some of which appear to originate from splitting between the two innermost myelin lamellae at higher power. The frequent appearance of adaxonal vacuoles may underpin the role of intraoligodendroglial vacuolar change in the development of intramyelin vacuoles in mitochondrial encephalopathies such as KSS, as discussed later.

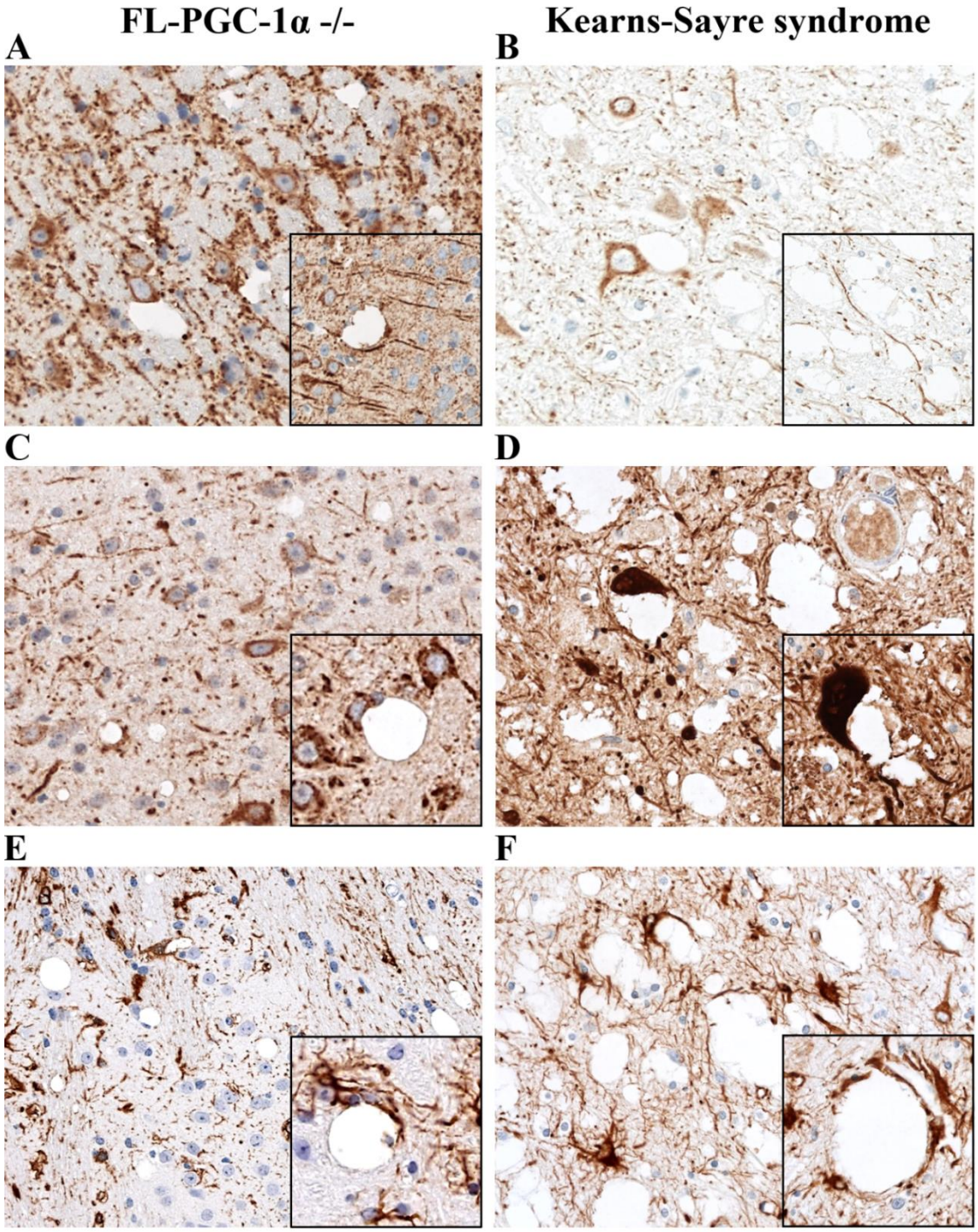

Figure 12. Rare findings of vacuoles being in close contact with structures positive for staining against neuronal (A–B, MAP-2**; C–D,** SMI-32**) or astroglial (E–F,** GFAP**) antigens.** Notably, the vast majority of GM neuropil vacuoles have no immunohistochemically detectable association with such structures, which are often merely pushed by vacuoles of most probably distinct origin.

V. DISCUSSION

With multiple links associating PGC-1α dysfunction with neurodegenerative diseases, especially HD, PGC-1α-deficient mice with consistent early reports on striatal vacuolation and astrocytosis are frequently referred to as animals exhibiting HD-like pathology and phenotype. Prompted by the facts that mitochondrial dysfunction and, though only at *in vitro* levels, PGC-1α deficiency has been causatively linked to pathological neuronal protein accumulation as a sign of impaired protein processing characteristic of neurodegenerative diseases, as well as by the notion that neither hyperactive behavior nor CNS vacuolation are typical features of mammalians with HD, we performed a systematic neuropathological mapping of the brain of FL-PGC-1α -/- animals.

As regards neurodegeneration-related proteins, our immunohistochemical analysis revealed no protein depositions, with a complete lack of tangle-like structures, extracellular plaques, and ubiquitin-immunopositive inclusion bodies throughout the 30-week-old murine brains. Notably, the same set of immunohistochemical stainings performed on remarkably more aged, 70-75-week-old, FL-PGC-1α -/- mice, revealed identical physiological patterns. These results indicate that despite its widely established contribution in neurodegenerative diseases, the absence of FL-PGC-1α has no major influence on protein processing in mice, suggesting a more complex scenario for the interaction of mitochondrial dysfunction and protein aggregation in such conditions.

During neuropathological profiling, alterations in FL-PGC-1α -/- mice consisted of widespread spongiform vacuolation and circumscribed astrogliosis. The observed pattern was highly reminiscent of human mitochondrial spongiform encephalopathies, particularly of KSS (Table 2), but not of HD or any other 'classical' neurodegenerative disorders. The relevance of the characterization of a viable animal model with mitochondrial encephalopathy is potentially striking, as previous attempts to create valid animal tools to model such diseases have been facing difficulties. Indeed, most of the developed genetic modifications resulted in embryonic or early postnatal lethality, whereas a great proportion of viable strains, surprisingly, exhibit no neuropathology. To our knowledge, murine knockouts of apoptosis-inducing factor (AIF), SOD2, thymidine phosphorylase and uridine phosphorylase (TP/UP), and NADH dehydrogenase [ubiquinone] iron-sulfur protein 4 (NDUFS4) are the only ones that display a neuropathology resembling that of human mitochondrial encephalopathies (Table 2). The most closely reminiscent brain pathology of that observed in this study was reported in the murine knockout of SOD2 (also acting downstream of PGC-1α).

Disease	*Vacuolation*	*Anatomical predominance of vacuolation*	*Astrogliosis*	*Anatomical predominance of astrogliosis*
Human disorders				
KSS	+	cerebral WM thalamus basal ganglia brainstem cerebellum	+	brainstem cerebellum
LS	+	thalamus basal ganglia brainstem cerebellar nuclei	+	thalamus basal ganglia brainstem cerebellar nuclei
MELAS	+	cerebrum cerebellum	+	cerebrum thalamus basal ganglia brainstem cerebellum
MERRF	+	cerebrum brainstem	+	basal ganglia brainstem cerebellar cortex cerebellar nuclei
LHON	+	optic nerve	+	optic nerve retinal ganglia
Experimental models				
FL-PGC-1α -/- mice	+	cerebrum thalamus basal ganglia brainstem cerebellar nuclei	+	brainstem cerebellar nuclei
Ndufs4 -/- mice	+	brainstem cerebellar nuclei	+	brainstem cerebellar nuclei
TP/UP double -/- mice	+	cerebral WM thalamus basal ganglia cerebellar WM cerebellar nuclei	No data available	
SOD-2 -/- mice	+	cerebral cortex brainstem	+	cerebral cortex brainstem
AIF -/- (Harlequin) mice	-		+	thalamus basal ganglia cerebellar nuclei retinal ganglia optic tract

Table 2. Comparative summary of the typical neuropathological findings and their distribution in human mitochondrial spongiform encephalopathies and their most reminiscent murine models.

The possibility that PGC-1α-deficient mice could represent a useful animal model of this intractable group of diseases prompted us to perform a step-by-step comparison of aged 70-75-week-old FL-PGC-1α -/- mice and a human case of KSS, with special focus on the origin of vacuoles. Our analysis revealed that vacuolation in FL-PGC-1α -/- mice is predominantly localized within the myelin sheath in the absence of morphological signs of axonal and scattered indications of astroglial or neuronal involvement. The findings were altogether strikingly similar to that seen in KSS, with a remarkable difference being that in KSS, the devastatingly vacuolated (cystic-necrotic) lesions presented also with myelin pallor and axonal disintegration. The sparing of axons in FL-PGC-1α -/- mice contrasts the previous concept proposed during the initial characterization of PGC-1α -/- strain that vacuolation might arise from axonal degeneration. Furthermore, the consistent lack of reactive astrocytes in the striatum even at an old age repeatedly questions the concept that PGC-1α-deficient animals might indeed be models of HD. Notably, an independent group performing parallel examinations on complete PGC-1α -/- mice reported no significant striatal neurodegeneration but reported a significant loss of cerebellar Purkinje neurons, which is striking, as this feature is virtually pathognomonic of KSS.

In addition to being the first systematic comparison of human and animal mitochondrial encephalopathy, this part of our study provided two main novelties. First it demonstrates commonalities of vacuolation in the WM and GM, placing oligodendrocytes in the center of disease pathogenesis. Indeed, though WM vacuoles have been generally presumed to develop due to intramyelin edema secondary to mitochondrial dysfunction of oligodendrocytes, GM neuropil vacuoles have been proposed to develop due to ion transport disorder of astrocytic membranes. Our observation that the majority of GM neuropil vacuoles are clearly myelin-bound in both the KSS and FL-PGC-1α -/- brains indicates that the cellular localization and thus the mechanism of vacuole formation is most likely similar in both the WM and GM. Secondly, the ultrastructural analysis revealed the common appearance of intracellular, often multiloculated formation of vacuoles within oligodendroglial cells both in the KSS case and FL-PGC-1α -/- brains. This was supported by the immunohistochemical observation of TPPP/p25-positive oligodendrocytes directly attaching to and sometimes bulging into vacuoles within the neuropil. Interestingly, though intracellular oligodendroglial vacuoles have not been previously described in mitochondrial diseases, their presence is not unprecedented in pathologies associated with mitochondrial dysfunction and/or severe cellular stress. Among them, intoxication of mice with cuprizone, a copper-chelating mitochondrial toxin, evokes a CNS pathology strikingly similar to those observed in our study, with vacuole formation due to

intraperiod line splitting in the pons, midbrain, thalamus, cerebral and cerebellar WM, and the deep cortical layers, along with the presence of oligodendrocytes with enlarged cytoplasm containing multiloculated vesicles.

Although the potential role of oligodendrocytes in WM vacuolation in mitochondrial encephalopathies has already been suggested, the fundamental concepts included 1) a disrupted ion-homeostasis of the sheath, 2) a dysfunction of the blood-brain barrier, in both cases with consequent development of 'intramyelin edema'. These hypotheses, however, do not explain why vacuoles develop focally and how multiple vacuoles can be found within the same internode, instead of a complete splitting and diffuse loosening of the sheath between all lamellae. We propose that chronic mitochondrial dysfunction in a yet unknown pathway leads to the formation of multiple intraoligodendroglial fluid-filled vacuoles. The increased intracellular content might provoke splitting between the intracellular surfaces of the myelin sheath (major dense line). Due to their firm connections at the macromolecular level, this would cause tears and focal myelin disruptions, allowing the vacuolar content to access into the virtual space between the loosely attached extracellular surfaces (intraperiod lines). Consequently, this could evoke the formation of focal splits and eventually myelin bubbles. Accordingly, disruption of the lateral loops or probably of some developmental remnants of the cytoplasmic incisures would result in intraperiod line splitting at the corresponding levels, whereas leakage from the inner tongue would cause adaxonal swelling between the axolemma and the innermost myelin lamellae or between the two innermost layers. Supporting this theoretical consideration, such distinct types of intramyelin vacuoles have indeed been described in experimental status spongiosus, and could also be observed in our study (Figure 11). Our observations, therefore, place oligodendrocytes in the center of the pathogenesis of CNS lesioning in association with chronic mitochondrial dysfunction, which is in line with the recognition that oligodendrocytes are most sensitive to mitochondrial stress, exceeding the vulnerability of neurons.

VI. CONCLUSION

We systematically characterized the neuropathological alterations of FL-PGC-1α -/- mice. Providing evidence that these animals do not associate with morphological features of neurodegenerative diseases, including HD, we reported the characterization of a phenotype strikingly reminiscent of that seen in mitochondrial encephalopathies, especially in KSS. Extending our investigations to further immunohistochemical and ultrastructural levels in a systematic comparison with the human disease, we identified novel pathological alterations

present in both human KSS and FL-PGC-1α -/- animals, providing basis of a novel generalized theory for vacuole formation in mitochondrial and probably other metabolic diseases. We propose that PGC-1α-deficient mice can be an appropriate animal model for this yet incurable group of diseases, and should be subjected to examination with therapeutic aim.

VII. ACKNOWLEDGEMENTS

I am grateful to Máte Molnár, Rita Török, Dénes Zádori, Pawel P. Liberski, László Vécsei, Gábor G. Kovács, and Péter Klivényi for their valuable contribution. The studies included in the thesis were supported by the National Brain Research Program (KTIA_NAP_13-A_II/18), the European Union and the State of Hungary, co-financed by the European Social Fund in the framework of TÁMOP-4.2.4. A/2-11-1-2012-0001 ‘National Excellence Program’, TÁMOP-4.2.2/B-10/1-2010-0012, and TÁMOP-4.2.2.A-11/1/KONV-2012-0052.